Imaging Noisy Seismic Data using a One Dimensional Inverse Scattering Algorithm

Bogdan G. Nita & Christopher Smith
Department of Mathematical Sciences, Montclair State University, Montclair, NJ

Student: chris.smith324@gmail.com
Mentor: nitab@mail.montclair.edu

ABSTRACT
We test the capability of an inverse scattering algorithm for imaging noisy seismic data. The algorithm does not require a velocity model or any other a priori information about the medium under investigation. We use three different geometries which capture different types of one-dimensional media with variable velocity. We show that the algorithm can precisely locate the interfaces and discover the correct velocity changes at those interfaces under moderate noise condition. When the signal to noise ratio is too small, the data is de-noised using a threshold filter and then imaged with excellent results.

KEYWORDS
Seismic Imaging, Inversion, Amplitude Correction, Scattering Theory, Noise, Threshold Filter.
2000 MATHEMATICS SUBJECT CLASSIFICATION 86A22, 35J05, 35R30.

1. INTRODUCTION

Inverse scattering theory is a framework for determining the characteristics of an object from measurement data of waves or particles scattered from that object. In contrast to other imaging methods, no a priori information about the object or about the medium surrounding the object is necessary to extract the location and the characteristics of the object. This makes inverse scattering theory a very unique tool, presently being the only direct method with this capability. The application of inverse scattering methods to seismic exploration has been extensively discussed in the literature (see for example [1] and [2] and the references therein).[1,2] In 2009, Nita[3] found an inverse scattering algorithm for simultaneous imaging and inversion which was recently tested numerically with excellent results.[4]

The data recorded in a seismic experiment contain several types of arrivals like primary reflections, multiple reflections, free surface multiple reflections, source and receiver ghost waves, direct wave from the source, ambient noise and others depending on the location of the receivers.[6] Out of these, only primary reflections are considered useful signal and all current imaging algorithms are designed to process only this small part of the data.[7] Any other type of signal is considered noise and consequently eliminated, totally or partially, in a pre-processing phase.

The unwanted part of the data can be further split into two categories: coherent and random noise. Coherent noise usually consists of multiple reflections of the initial wave and many algorithms exist today to attenuate or eliminate it.[8] In this paper, we test the capability of the inverse scattering algorithm using data contaminated with random noise. We use various earth models to capture the characteristics of several earth configurations (different number of layers, different velocity contrasts and velocity inversions). For consistency and comparison purposes we use the same models as did Tasy.[4] Following the standard seismic industry pre-processing steps, we assume that the source signature has been deconvolved from the data and that all coherent noise has been eliminated. Therefore, the data that we use in our imaging algorithm only consists of single (primary) reflections and random noise.

2. BACKGROUND

In this section we briefly describe the theory behind the algorithm that we will be testing. We start with the equation describing the acoustic wave propagation in a 1-D constant density variable velocity medium

$$\left(\frac{d^2}{dz^2} + k^2(z)\right) P(z, \omega) = 0 \quad \textbf{Equation 2.1}$$

where P is the pressure field at depth z, $k(z) = \omega/c(z)$ is the vertical wavenumber, ω the angular frequency and $c(z)$ the velocity of sound in the medium. This equation does not include a source term and hence it only models the propagation of an existing waveform and not how the waveform is created. Assume a reference medium represented by an acoustic wholespace with velocity c_0, and define a perturbation operator[1]

$$V = k_0^2 \alpha(z) \quad \textbf{Equation 2.2}$$

where $k_0 = \frac{w}{c_0}$ and $\alpha(z) = 1 - \frac{c_0^2}{c^2(z)}$. In this framework, the inverse problem is to solve for α which in turn will provide information about the velocity in the unknown medium, $c(z)$. The inverse scattering series is a power series containing powers of the collected data and, for this problem (one dimensional medium with one parameter — velocity), it takes the form

$$\alpha(z) = \alpha_1(z) + \alpha_2(z) + \alpha_3(z) + \ldots \quad \textbf{Equation 2.3}$$

where $\alpha_i(z)$ for any $i \geq 1$ contains the $i - th$ power of the data.

After solving for the first few terms in the series, and identifying them as either imaging or inversion driving terms[5] one can select the desired pieces and group them in a subseries which only performs a targeted task: free surface or internal multiple attenuation, imaging or inversion. Such a subseries for simultaneous imaging and inversion was discovered[3] which showed that the respective series is convergent for all values of the perturbation operator and the limit is,

$$\alpha^{SII}(z) = \int_{-\infty}^{\infty} e^{ik_0 z} \int_{-\infty}^{\infty} \alpha_1(z') e^{-ik_0\left(z' + \frac{1}{2}\int_{-\infty}^{z'} \alpha_1(z'')dz''\right)} dz' dk_0. \quad \textbf{Equation 2.4}$$

This is the closed form of the subseries for imaging and inversion which will be tested numerically in this paper with noisy seismic data. As mentioned before, the algorithm assumes that multiples have been removed from the data (in addition to source signature and ghosts) and therefore the data only contains primaries.

Although **Equation 2.4** describes only a 1-D algorithm, this algorithm promises the recovery of an image of the actual medium from collected data and knowledge of a reference medium only, without a velocity model or any other assumption about the medium under investigation. All other seismic exploration imaging techniques are dependent on some a priori assumption about the targeted medium.[9]

3. NUMERICAL TESTS FOR THE SIMULTANEOUS IMAGING AND INVERSION ALGORITHM

In this chapter we test the Simultaneous Imaging and Inversion Algorithm using several data sets collected over three earth models. All numerical tests were performed on a Desktop PC using MAPLE. For each earth model we have to first create the geometry (layers and corresponding velocities), then simulate a seismic experiment to create the data, and finally corrupt this data with random noise. The data is then ran through the imaging algorithm (**Equation 2.4**) and the image is compared with the initial model. We will observe two main characteristics of the algorithm: its ability to correctly find the depths of the interfaces of the unknown media and its ability to determine the correct amplitudes in the perturbation operator.

3.1 MODEL 1: MONOTONIC INCREASING VELOCITY

The first model consists of three interfaces located in water at depths of z_1 = 100, z_2 = 130, and z_3 = 160 with the sound velocity inside of the layers having the values c_0 = 1500, c_1 = 1650, c_2 = 1725, and c_3 = 1800 (see **Figure 1a**). The perturbation operator, α, for this earth model is shown in **Figure 1b**. The data in this case consists of three primary reflections shown in **Figure 1c**. The output of the algorithm is shown in blue in **Figure 1d** and it is easily compared with the actual model (in red) and with the first approximation α_1 in green.

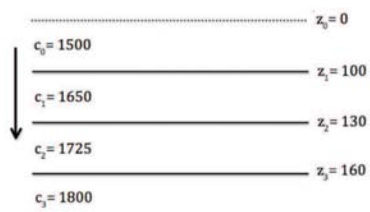

(a) Earth Model 1

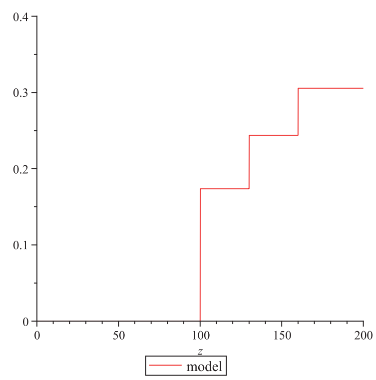

(b) Perturbation Operator for Model 1

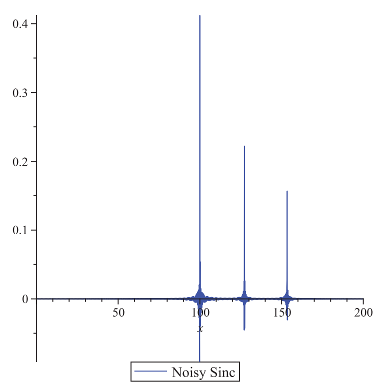

(c) Model 1 no noise data

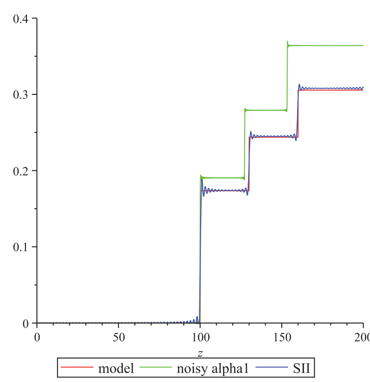

(d) Model 1 no noise image

Figure 1. Model 1 imaging algorithm using noise free data

We incrementally add noise to the data (with a standard deviation STD ranging from 0.001 to 0.01), see **Figures 2a, 2c, 2e** and notice how the image produced by the algorithm deteriorates in **Figures 2b, 2d, 2f**.

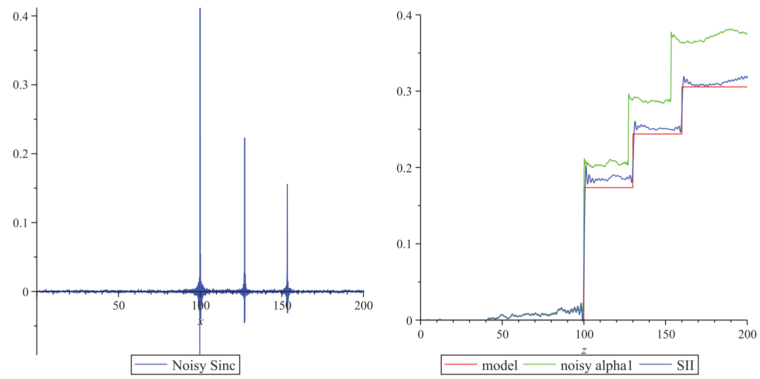

(a) Model 1 STD 0.001 noise data (b) Model 1 STD 0.001 noise image

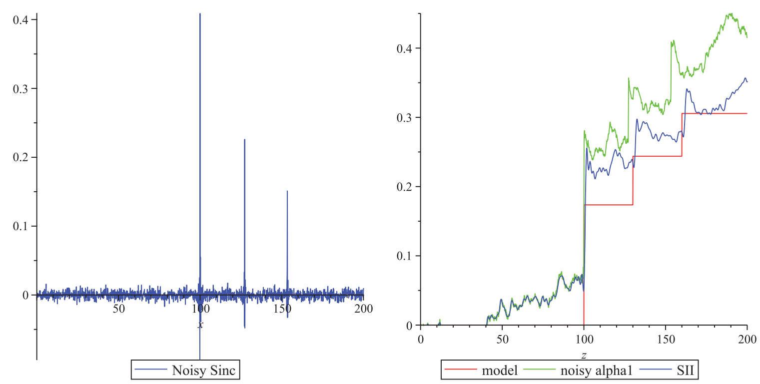

(c) Model 1 STD 0.005 noise data (d) Model 1 STD 0.005 noise image

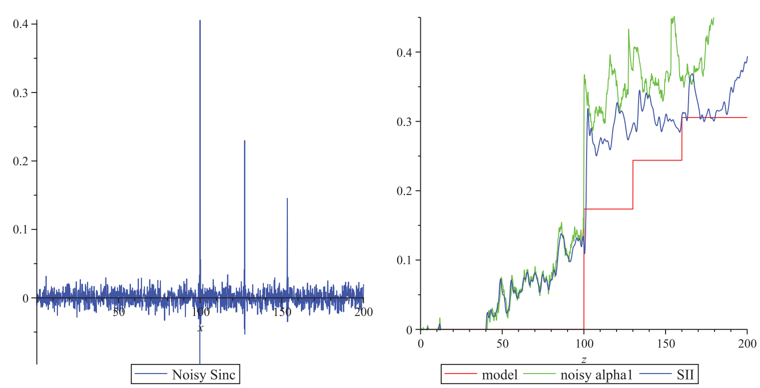

(e) Model 1 STD 0.01 noise data (f) Model 1 STD 0.01 noise image

Figure 2. Model 1 imaging algorithm with increasingly more noise

Not surprisingly, the high level of random noise in the data affects the image negatively. Following the common seismic processing practice, we proceed by applying a filter to the data to clean up some of this noise. There are many types of filters that can be used to attenuate or eliminate random noise. For example one can use non-causal prediction filters,[10] adaptive filters[11] or some transform methods like seislet transform,[12] discrete cosine transform[13] and curvelet transform[14] to improve the signal to noise ratio. Due to the nature of this project, we decided on a simpler threshold filter which practically mutes all signal with an amplitude less than 0.05 (see **Figures 3a, 3c, 3e**). We then use the algorithm on the filtered data and obtain the images shown in **Figures 3b, 3d, 3f**.

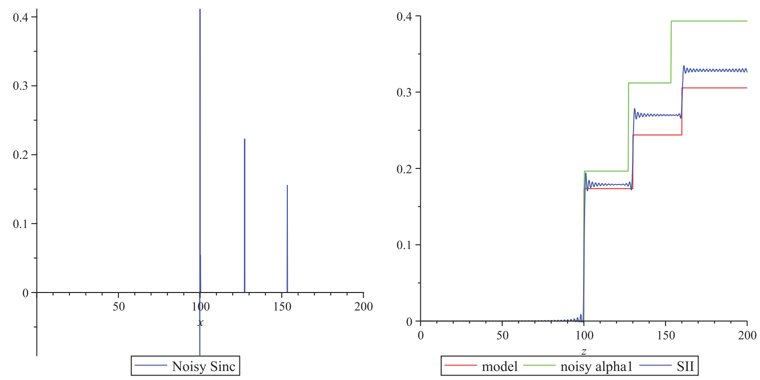

(a) Model 1 STD 0.001 noise filtered data (b) Model 1 STD 0.001 noise filtered image

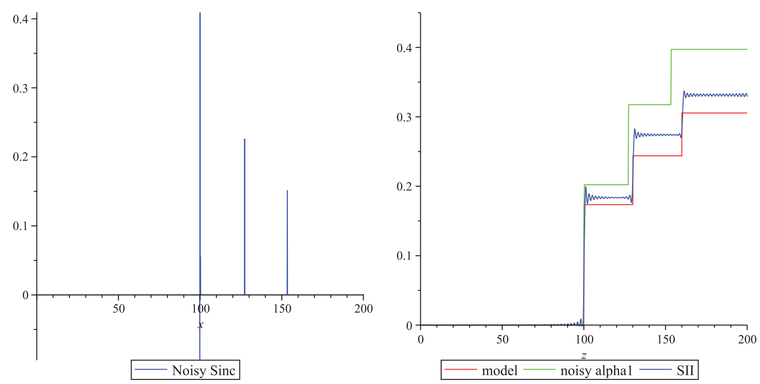

(c) Model 1 STD 0.005 noise filtered data (d) Model 1 STD 0.005 noise filtered image

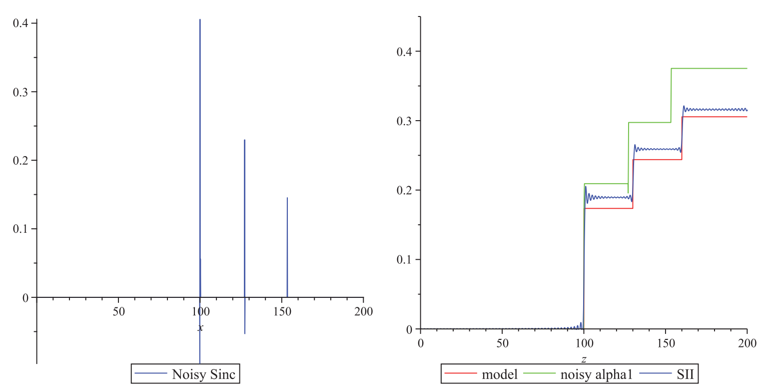

(e) Model 1 STD 0.01 noise filtered data (f) Model 1 STD 0.01 noise filtered image

Figure 3. Model 1 imaging algorithm with increasingly more noise

The obtained results show that the algorithm is stable and capable of reproducing the correct location of the interfaces even after significant noise contamination. We notice that some amplitude information is lost due to the noise and the applied filter; however this could be improved by using a more complex filtering method.

3.2 MODEL 2: NON-MONOTONIC VELOCITY

The second model consists of four interfaces located in water at depths of $z_1 = 100$, $z_2 = 130$, $z_3 = 160$ and $z_4 = 200$ with the sound velocity inside of the layers having the values $c_0 = 1500$, $c_1 = 1650$, $c_2 = 1725$, $c_3 = 1575$ and $c_4 = 1725$ (See **Figure 4a**). This model is important to examine because, unlike the first example, the velocities in the layers are no longer monotonic. The perturbation operator

for this earth model is shown in **Figure 4b**. The data in this case consists of four primary refl ections shown in **Figure 4c**. Notice that the third spike in the data, corresponding to the primary reflection off the third interface, is negative. This is because, at the third interface, the velocity in the deeper layer is less then the velocity in the shallower layer. The output of the algorithm is shown in blue in **Figure 4d** together with the actual model (in red) and with the first approximation α_1 in green.

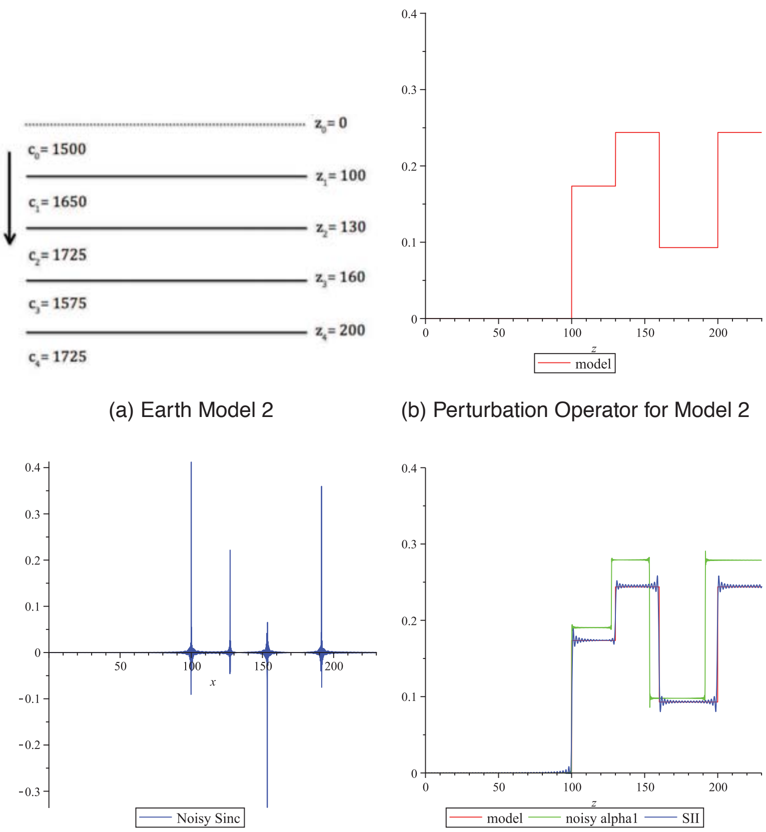

(a) Earth Model 2 (b) Perturbation Operator for Model 2

(c) Model 2 no noise data (d) Model 2 no noise image

Figure 4. Model 2 imaging algorithm using noise free data

As before we add noise to the data, with a standard deviation ranging from 0.001 to 0.01 (see **Figures 5a, 5c, 5e**). As expected, the image produced by the algorithm becomes distorted and makes it very difficult to extract any useful information from it (see **Figures 5b, 5d, 5f**).

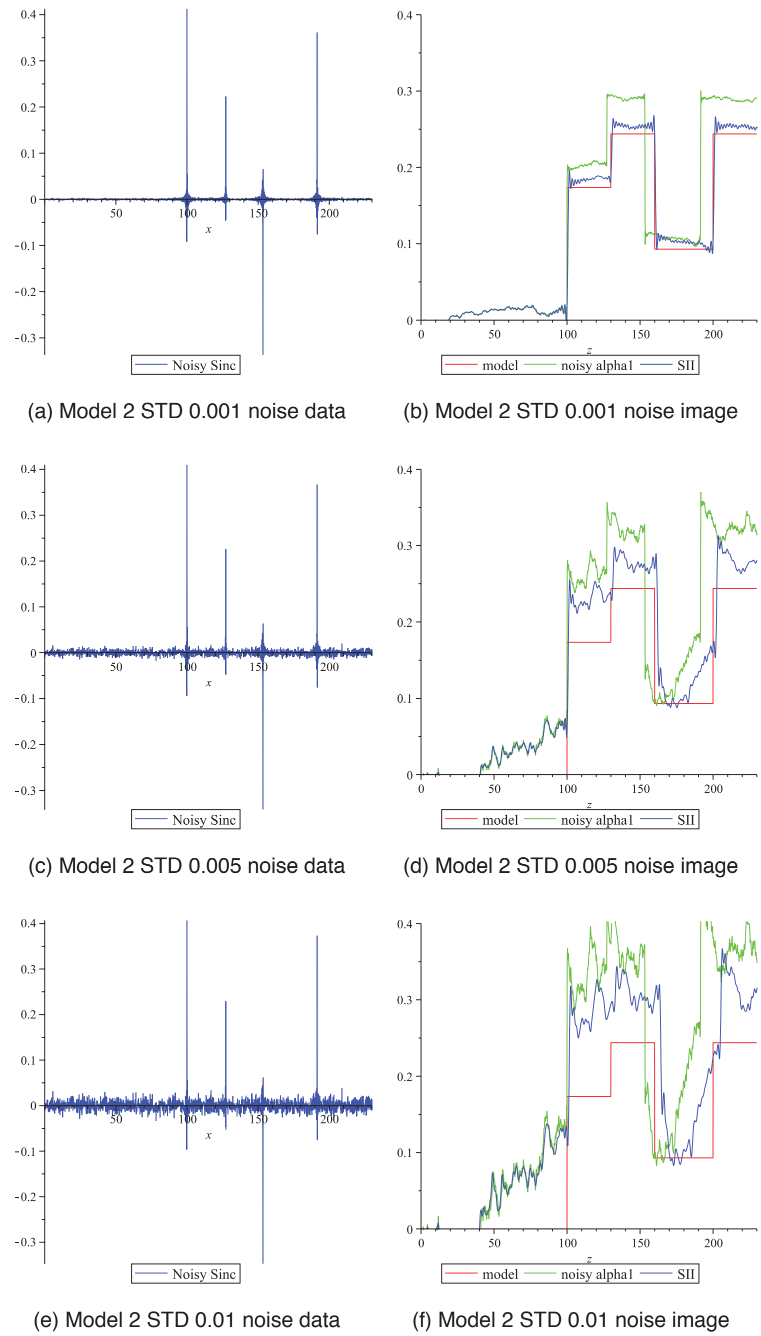

(a) Model 2 STD 0.001 noise data (b) Model 2 STD 0.001 noise image

(c) Model 2 STD 0.005 noise data (d) Model 2 STD 0.005 noise image

(e) Model 2 STD 0.01 noise data (f) Model 2 STD 0.01 noise image

Figure 5. Model 2 imaging algorithm with increasingly more noise

After applying the same threshold filter as before (see **Figures 6a, 6c, 6e**), the image clears up and, although some amplitude information is lost, the interfaces of the model are clearly delineated for all three levels of noise (see **Figures 6b, 6d, 6f**). In conclusion, for this second model, the combination of data filtering and inverse scattering algorithm works very well.

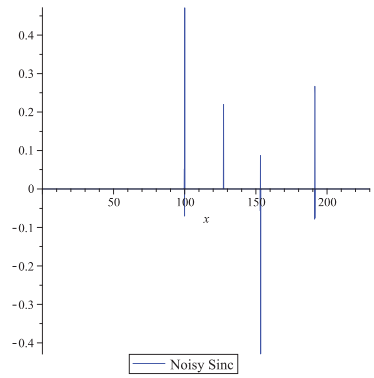

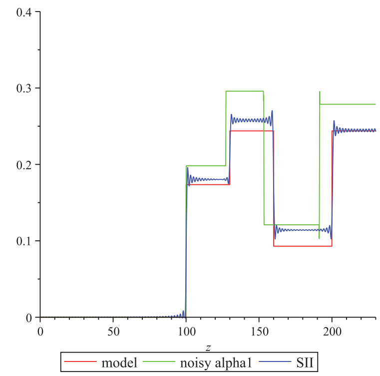

(a) Model 2 STD 0.001 noise filtered data (b) Model 2 STD 0.001 noise filtered image

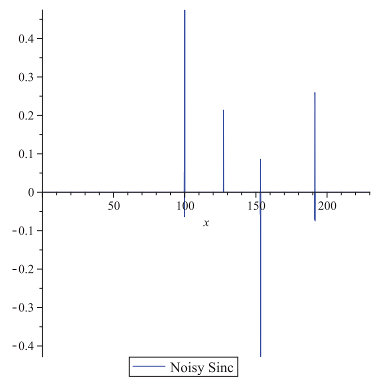

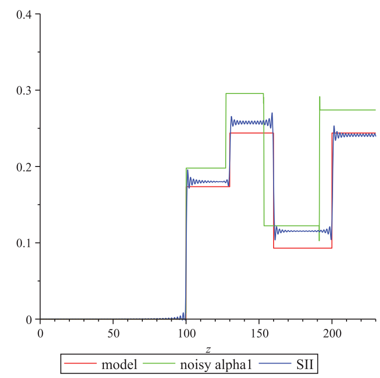

(c) Model 2 STD 0.005 noise filtered data (d) Model 2 STD 0.005 noise filtered image

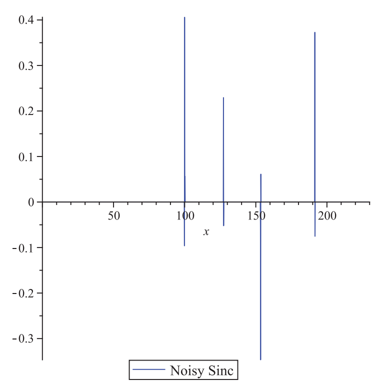

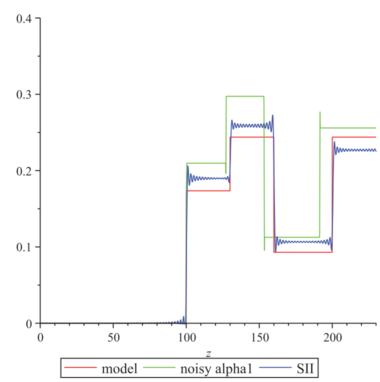

(e) Model 2 STD 0.01 noise filtered data (f) Model 2 STD 0.01 noise filtered image

Figure 6. Model 2 imaging algorithm with increasingly more noise

3.3 MODEL 3: OSCILLATING VELOCITY

The third model consists of six interfaces located in water at depths of z_1 = 100, z_2 = 130, z_3 = 160, z_4 = 200, z_5 = 240, and z_6 = 260 with the sound velocity inside of the layers having the values c_0 = 1500 and then alternating between 1850 and 1625, respectively (see **Figure 7a**). This model is important to examine because it contains several velocity inversions and large velocity contrasts. The perturbation operator for this earth model is shown in **Figure 7b**. The data in this case consists of six primary reflections plotted in the depth domain in **Figure 7c**. Notice that the pulses alternate between positive and negative amplitude, which is consistent with the alternating velocity inversions in the model. The output of the algorithm is shown in blue in **Figure 7d** together with the actual model (in red) and with the first approximation α_1 in green.

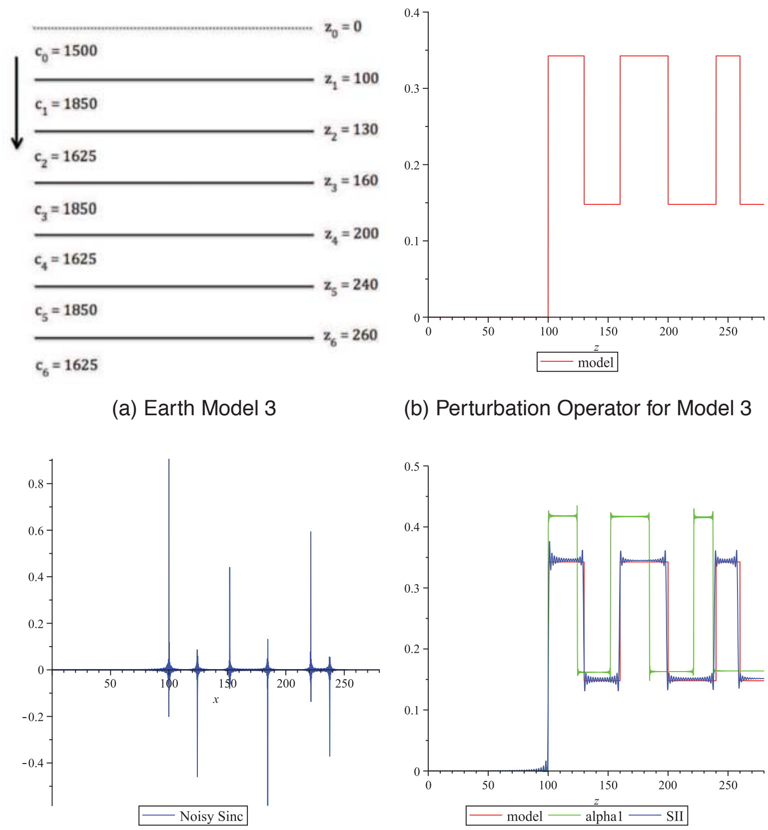

(a) Earth Model 3

(b) Perturbation Operator for Model 3

(c) Model 3 no noise data

(d) Model 3 no noise image

Figure 7. Model 3 imaging algorithm using noise free data

In the next step we add noise to the data, with the same standard deviation as before (see **Figures 8a, 8c, 8e**). The image produced by the algorithm deteriorates accordingly as it can be seen in **Figures 8b, 8d, 8f.**

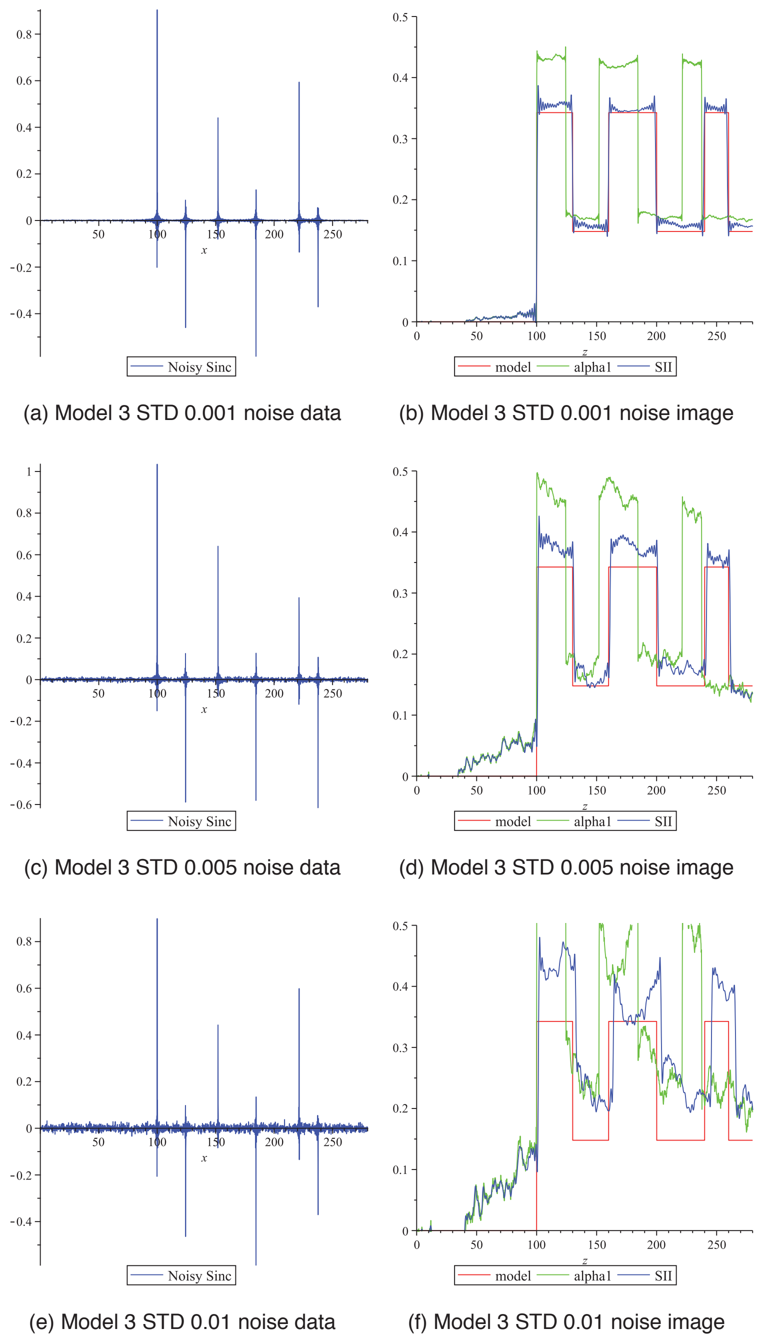

(a) Model 3 STD 0.001 noise data (b) Model 3 STD 0.001 noise image

(c) Model 3 STD 0.005 noise data (d) Model 3 STD 0.005 noise image

(e) Model 3 STD 0.01 noise data (f) Model 3 STD 0.01 noise image

Figure 8. Model 3 imaging algorithm with increasingly more noise

Filtering the noise using the same threshold filters cleans up the data as seen in **Figures 9a, 9c, 9e**but it also results in some loss of amplitude information in the final image (see **Figures 9b, 9d, 9f**). We notice however that the algorithm places all interfaces at their exact location.

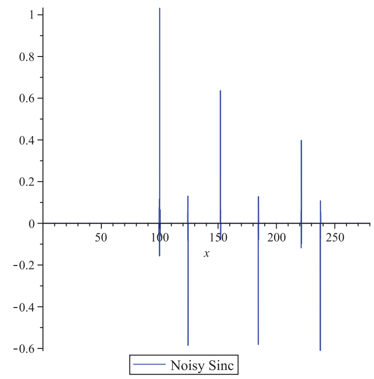

(a) Model 3 STD 0.001 noise filtered data

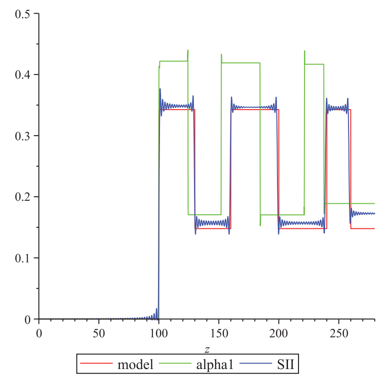

(b) Model 3 STD 0.001 noise filtered image

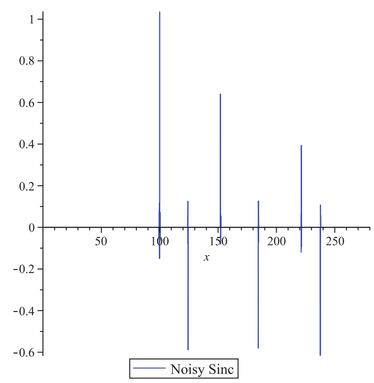

(c) Model 3 STD 0.005 noise filtered data

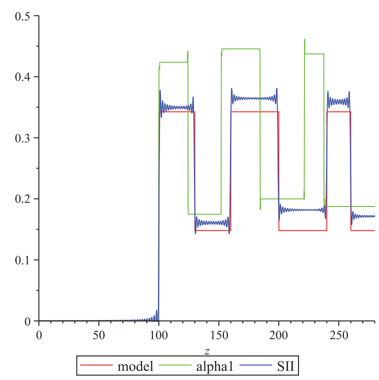

(d) Model 3 STD 0.005 noise filtered image

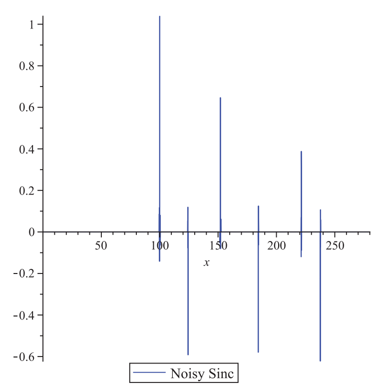

(e) Model 3 STD 0.01 noise filtered data

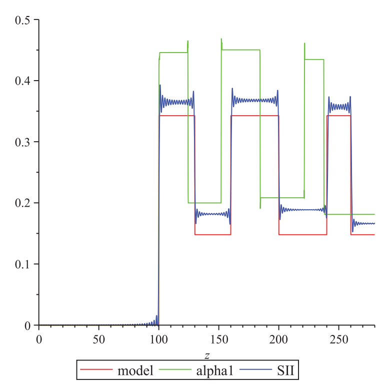

(f) Model 3 STD 0.01 noise filtered image

Figure 9. Model 3 imaging algorithm with increasingly more noise

4. CONCLUSION

In this paper, we tested the capability of an inverse scattering algorithm for imaging seismic data. The algorithm we investigated simultaneously images and inverts one-dimensional, one-parameter (velocity), acoustic reflection data. The algorithm does not require a velocity model or any other a priori information about the medium under investigation, the only input being a reference velocity (the speed of sound in water in this case) and the data collected in the experiment.

In our tests, we used three earth models and data which was corrupted by random noise of different magnitudes. These choices of earth models exemplify different conditions that can be found in a one-dimensional medium with variable velocity. As the level of noise was increased, we noticed that the image produced by the algorithm was deteriorating. Following standard seismic processing techniques, we applied a simple threshold filter to mute any signal with an amplitude lower than 0.05. This filter removed all the random noise but also some of the signal used in the imaging algorithm. After running the filtered data through the imaging algorithm, we noticed that the location of the interfaces of the seismic models were still perfectly located. The amplitude was also recovered satisfactorily although the noise and the applied filters affected the final image somewhat.

These results are promising and warrant further research. Some of the planned future work includes imaging data with missing low frequencies and extending the algorithm to 1.5 and 2-dimensional media.

ACKNOWLEDGMENTS

This material is based on work supported by the National Science Foundation's REU Program IIS-1004447 and grants MRI-0959461 and CNS-0922644. Any opinions, findings, and conclusions or recommendations expressed in this material are those of the author(s) and do not necessarily reflect the views of the NSF.

REFERENCES

[1] Weglein, A.B., Araujo, F.V., Carvalho, P.M., Stolt, R.H., Matson, K.H., Coats, R.T., Corrigan, D., Foster, D.J., Shaw, S.A. and Zhang, H. (2003). Inverse scattering series and seismic exploration, Inverse Problems 19(6): R27R83.

[2] Soriano, K., Oonlamom, T. and Nita, B.G. (2013). Imaging seismic data using inverse scattering theory, International Journal of Tomography and Simulation 23(2): 19.

[3] Nita, B.G. (2009). An algorithm for seismic imaging and amplitude correction derived from scattering theory, International Journal of Tomography and Statistics 11(SO9): 118133.

[4] Tasy, A., Santamaria, G. and Nita, B.G. (2013). Numerical evaluation of a one dimensional in- verse scattering algorithm for simultaneous seismic imaging and inversion, Applied Mathematics and Computation 219(10): 50495069.

[5] Shaw, S.A. (2005). An inverse scattering series algorithm for depth imaging of reflection data from a layered acoustic medium with an unknown velocity model, Ph.D. Thesis, University of Houston, TX.

[6] Kearey, P., Brooks, M., Hill, I. (2002). An Introduction to Geophysical Exploration, Wiley-Blackwell. 3rd edition.

[7] Yilmaz, O. (2001). Seismic Data Analysis: Processing, Inversion and Interpretation of Seismic Data, Society of Exploration Geophysicists. 2nd edition.

[8] Weglein, A.B., Dragoset, W.H (2005). Multiple Attenuation, Society Of Exploration Geophysicists.

[9] Stolt, R.H., Weglein A.B. (2012). Seismic Imaging and Inversion, Cambridge University Press.

[10] Gulunay, N. (2000). Noncausal spatial prediction filtering for random noise reduction on 3-D post-stack data: Geophysics,65, 1641–1653.

[11] Ristau, J.P., Moon, W.M. (2001). Adaptive filtering of random noise in 2-D geophysical data: Geophysics, 66, 342–349.

[12] Fomel, S., Liu, Y. (2008). Seismic data analysis with one-dimensional seislet frame: 78th Annual International Meeting, SEG, Expanded Abstracts, 2581–2585.

[13] Lu, W., Liu, J (2007). Random noise suppression based on discrete cosine transform: 77th Annual International Meeting, SEG, Expanded Abstracts, 2668–2672.

[14] (Neelamani et al., 2008). Neelamani, R., Baumstein, A.I., Gillard, D.G., Hadidi, M.T., Soroka, W.I. (2008). Coherent and random noise attenuation using the curvelet transform: The Leading Edge, 27, 240–248.

ABOUT THE STUDENT AUTHOR

Christopher Smith graduated from The College of New Jersey in 2012 with a BS in Computer Science. He is now a Software Engineer at ZocDoc, NY. The work in this paper was completed while enrolled in the NSF funded REU program iMagine in the Computer Science Department at Montclair State University.

PRESS SUMMARY

All imaging procedures (from seismic exploration to medical) assume a velocity model for their targeted media. For example, medical ultrasound assumes that human body is made out of water and therefore sound waves that traverse it propagate with a speed of 1500m/s. Seismic exploration methods also assume a more complex velocity model, which usually is inaccurate and produces false images of the subsurface. Inverse scattering theory provides an infrastructure that makes possible imaging without these initial assumptions. In this paper we present such an algorithm and show its ability to image noisy data.